Experiments in Fluids 25 (1998) 491–502 © Springer-Verlag 1998

Laminarisation and re-transition of a turbulent boundary layer subjected to favourable pressure gradient

M. P. Escudier, A. Abdel-Hameed, M. W. Johnson, C. J. Sutcliffe

Abstract Experimental results are reported for the response of an initially turbulent boundary layer ($Re_\theta \approx 1700$) to a favourable pressure gradient with a peak value of $K \equiv (-\upsilon/\rho U_E^3)\, \mathrm{d}p/\mathrm{d}x$ equal to 4.4×10^{-6}. In the near-wall region of the boundary layer ($y/\delta < 0.1$) the turbulence intensity u' scales roughly with the free-stream velocity U_E until close to the location where K is a maximum whereas in the outer region u' remains essentially frozen. Once the pressure gradient is relaxed, the turbulence level increases throughout the boundary layer until K falls to zero when the near wall u' levels show a significant decrease. The intermittency γ is the clearest indicator of a fundamental change in the turbulence structure: once K exceeds 3×10^{-6}, the value of γ in the immediate vicinity of the wall γ_s falls rapidly from unity, reaches zero at the location where K again falls below 3×10^{-6} and then rises back to unity. Although γ is practically zero throughout the boundary layer in the vicinity of $\gamma_s = 0$, the turbulence level remains high. The explanation for what appears to be a contradiction is that the turbulent frequencies are too low to induce turbulent mixing. The mean velocity profile changes shape abruptly where K exceeds 3×10^{-6}. Values for the skin friction coefficient, based upon hot-film measurements, peak at the same location as K and fall to a minimum close to the location where K drops back to zero.

1 Introduction

A turbulent boundary layer subjected to streamwise acceleration of sufficient magnitude converts to a state which has some of the characteristics of a laminar boundary layer. Once the pressure gradient is relaxed the boundary layer reverts to a form which has a structure more typical of a turbulent flow. Since the structure of such laminarizing boundary layers undergoes major changes with streamwise location, it has long been recognised (e.g. Jones and Launder 1972) that it is unrealistic to expect that the magnitude of a single (pressure-gradient) parameter could control the onset of laminarisation. Nevertheless it is well established that if the value of the pressure-gradient parameter

$$K = -\frac{\upsilon}{\rho U_E^3}\frac{\mathrm{d}p}{\mathrm{d}x}.$$

exceeds about 3×10^{-6} laminarisation will eventually ensue although as Sreenivasan (1982), amongst others, has pointed out this particular parameter suffers from the major deficiency that it takes no cognisance of the boundary layer the laminarisation of which it is supposed to characterise. An elementary one-dimensional analysis of incompressible flow between converging flat surfaces produces the result

$$K = \frac{\upsilon}{U_E x}.$$

If x is of order 1 m, the value of U_E must be less than 5 m/s for an airflow to produce $K > 3 \times 10^{-6}$, and even lower velocities are needed if the scale is increased. A smaller scale, on the other hand, leads to higher velocities and more comfortable experimental conditions at the start of the acceleration, but also to very high velocities and thin boundary layers in the downstream region. This simple analysis suggests at least one reason why so few laminarisation experiments have been reported in the literature: the upstream flow velocities involved are inevitably so low and the downstream layers so thin that such experiments are difficult to perform. The review article of Sreenivasan (1982) lists only 14 experimental studies, none of them entirely satisfactory, and little would be added to such a review were it written today.

In the present paper we report on a laminarisation experiment in which particular attention was paid to a number of details. First, the contraction shape used to produce the acceleration, and hence $K(x)$, was based on the analytical solution for flow of an inviscid fluid over a forward-facing step. Second, the wall shear stress was determined from a surface hot-film at the same streamwise locations as the velocity and turbulence-intensity profiles over the 2.2 m stretch of the test plate. The wall shear stress is obviously a key parameter for any wall-shear flow but was identified as a deficiency in almost all of the experiments reviewed by Sreenivasan (1982). Another quantity subject to considerable uncertainty but clearly of

Received: *28 January 1998/Accepted*: *8 April 1998*

M. P. Escudier, A. Abdel-Hameed, M. W. Johnson, C. J. Sutcliffe
Department of Engineering: Mechanical Engineering
University of Liverpool
Liverpool L69 3 BX, U.K.

Correspondence to: M. P. Escudier

This research was carried out under Defence Research Agency contract reference CB/RAE/9/4/2067/068/RAE and was supported by the UK Department of Trade and Industry. The authors gratefully acknowledge this support and the encouragement of Dr P. R. Ashill and Ms C. J. Betts of DRA, Bedford.

major significance in any "transition" experiment is intermittency: the present work takes advantage of recent advances in the estimation of intermittency suggested by Johnson (1988). The study reported here provides considerably more detail than the comparable investigation of Blackwelder and Kovasznay (1972) about a number of aspects of the laminarisation/retransition process, particularly the latter.

2
Experimental equipment and procedures

The measurements were carried out in a low-speed open-return wind tunnel, designed by Gibson (1960) and described briefly in Bradshaw and Pankhurst (1964), modified for the present study by replacement of the original screen and paper honeycomb by six fine-mesh screens (United Wire 24 mesh 0.25 mm dia 58% free area) and an aluminium alloy honeycomb (Ciba-Geigy "Aeroweb" Type 3003 (2.3 $-\frac{3}{8}''$–15) 3″ thick). These new screens and honeycomb are located in the octagonal settling chamber (2.9 m across the flats) which reduces to a rectangular 1.22 m by 0.61 m outlet (i.e. 9:35 contraction ratio). Additional flow conditioning was provided by Ciba-Geigy "Aeroweb" Type 5052 honeycomb (3.4–$\frac{1}{4}''$–15) 2″ thick, immediately followed by a United Wire screen (10 mesh, 0.6 mm dia, 58% open area) installed between the fan and the settling chamber. Flow is produced by a 37.5 kW DC motor driving a four-bladed fan with radial inflow. The working section is 6 m in length with perspex sidewalls, a flat polished aluminium-alloy test plate (10 mm thick, 1.22 m wide with a 2 : 1 elliptical leading-edge profile), and a flexible roof made up of linked transverse slats (similar to a shutter blind) bonded to 1.5 mm thick rubber sheet. The roof shape is determined by the positions of a series of threaded rods which can be locked to two parallel beams running above and along the length of the working section. The initial shape of the contraction was based upon the analytical solution for flow over a forward facing step. Two solutions of the potential flow were examined, the initial analytical solution and an analytical solution with an applied bilinear transformation. The latter case was found to exhibit a steeper rise in K although the peak value of the distribution was the same for both cases. It was decided that the transformed distribution would be more suitable for the experiments because of its similarity to that corresponding to the flow over the leading edge of an aircraft wing (Ashill and Betts 1993) which was the principal motivation for the present work.

Pressure tappings (1 mm dia) are located along the centreline of the test plate at 100 mm pitch in the zero pressure gradient section and at 50 mm pitch, in two rows 25 mm either side of the centreline, and offset in the streamwise direction by 25 mm, in the acceleration section. Preliminary tests revealed that ambient temperature variations caused slow random pressure variations in the tubing connecting the pressure tappings to the differential pressure transducer (Baratron Model 270 signal conditioner with 698A11 TRA pressure head, range 10 Torr) used to measure the streamwise pressure distribution (and hence $\mathrm{d}p/\mathrm{d}x$ and K). This problem was overcome by routing all pressure tubing through 9 mm ID, 25 mm OD Armstrong "Armaflex" insulation tubing. The test plate is fixed 500 mm below the roof (109 mm above the lip) of the wind-tunnel outlet with a flap below the plate which is adjustable to ensure that the approach flow is aligned with the leading edge. A transverse row of 4 mm high, 2.4 mm dia. rivets with 5.2 mm dia flat heads (heads down), located 100 mm downstream of the leading edge (Blackwelder 1995), was provided to trip the boundary layer and produce a relatively thick, fully developed turbulent boundary layer prior to the acceleration zone.

Velocity and turbulence measurements were made using a single-wire boundary-layer probe (Dantec 9055P0151) with a Dantec M-series hot-wire anemometer system interfaced to a Microlink 3000 series data collection system comprising 3302 interface module, 3043 buffered 16 bit ADC, 3063 analogue input channel with anti-aliasing programmable filter and sample-and-hold circuitry, and 3070 rapid digitising module with external trigger. This system is interfaced via a Biodata IEEE 488 ISA communication board to a Ranger 486 33 MHz PC running Streamer software (Windmill Software Ltd) in MS Windows V3.1 environment. Preliminary experiments suggested that in order to properly resolve low-frequency fluctuations in the low-velocity approach flow, a sampling rate of 200 Hz was appropriate whereas for the high-frequencies typical of the high velocity flow resulting from the acceleration, a sampling frequency of 10 kHz was needed. To simplify operational procedures, it was decided to satisfy both criteria by sampling the hot-wire signals at 10 kHz for a period of 50 s thereby generating a data sample of 500,000 points for each flow condition.

The hot-wire probe was calibrated in a uniform airflow against a pitot-static tube for velocities in the range 2–25 m/s. For the range, 0.2–7 m/s, the calibration procedure of Lee and Budwig (1991) was followed whereby the frequency f of vortices shed from a wire (1.54, 2.79, 3.14 or 3.95 mm dia d) stretched across a uniform airflow was used to estimate velocity U from

$$St = 1.247 \times 10^{-4}\, Re + 0.1906 - 3.671/Re \quad \text{for } 50 < Re < 150$$

wherein

$$Re = Ud/\upsilon \text{ and } St = fd/U.$$

Temperature compensation covering the range 18–30 °C was introduced into the calibration according to the recommendations of Cimbala and Park (1990). The traverse system used for the velocity profile measurements had a resolution of 0.05 mm. Profiles consisted of measurements at 50 y-locations although obviously spurious points in the immediate vicinity of the surface were discarded (at most one in any profile). The only other correction made to the hot-wire measurements was an adjustment in the wire location to ensure that the mean velocity profile extrapolated linearly to zero at $y = 0$.

A system was developed which allowed a calibrated surface hot-film gauge (Dantec 55R47) to be moved along the centreline of the test plate to determine surface shear stress at any location and, in particular, at each location where a velocity profile was measured. The gauge was bonded to a semicircle of 100 μm thick polyester sheet held in place by a semicircular claw attached to the traverse also used (independently) for the hot-wire measurements. The polyester sheet was held in place by a thin film of oil beneath the sheet surrounding a polyester ring 50 μm thick and 37 mm dia which maintained the hot film

insulated from the test plate. The hot-film was calibrated against a set of Preston tubes assuming the calibration of Patel (1965) in a separate wind tunnel which could provide fully developed zero pressure gradient turbulent boundary layers over the appropriate range of shear stress. Friction factors were also determined using the Clauser (1954) method in the approach flow up to the location where $K = 1.85 \times 10^{-6}$, beyond which the velocity distribution deviated significantly from the logarithmic law, as well as from the wall slope of the mean velocity profile.

The algorithm used for determining intermittency γ is similar to that employed by Shaw et al. (1985) and is described in full in Johnson (1988) and Fasihfar (1992). Low frequencies characteristic of laminar instabilities are removed by applying a high pass digital filter set to a cutoff frequency $U_E/2\pi\delta$, a process which results in an intermittent high-frequency signal. A window of width $\pm u/10$ is then placed around the signal in order to discriminate between the laminar and turbulent parts of the signal. Whilst any part of the signal occurring outside the window is designated turbulent, it is incorrect to designate every point within the window as being laminar since the window may be crossed as a turbulent signal passes from peak to trough. In order to discriminate between turbulent signals crossing the window and genuine laminar portions of signal, a minimum residence time of $2\pi\delta/U_E$ is used. If the signal is within the window for a shorter period than this residence time it is designated turbulent whilst if the signal in inside the window for a longer period of time it is designated laminar.

3 Experimental results

3.1 Global and Integral quantities

Prior to discussing the more detailed measurements, it is instructive to consider the integral momentum thickness θ, the displacement thickness δ^*, the shape factor H, the skin-friction coefficient and other global quantities (Figs. 1 and 2) including various pressure-gradient parameters. At each location where wall pressure was measured, the pressure gradient was estimated by a linear fit through the three data points centred on that location. The corresponding streamwise variation of the pressure gradient parameter K is shown in Fig. 1, for an approach flow velocity U_o of 4 m/s. The peak value for K is 4.4×10^{-6} at $x = 4.1$ m, close to Blackwelder and Kovasznay's (1972) peak value of 4.8×10^{-6}. In the zone where the acceleration is strongest, it was found that there is a velocity gradient $\partial U_s/\partial y$ in the inviscid flow close to the test surface of the order 20 s^{-1}. A linear approximation was used for this variation of the inviscid flow velocity $U_s(y)$, determined from the measured velocity in the region $\delta \leqslant y \leqslant 1.4\ \delta$, and the integral thicknessses were then calculated from

$$\delta^* = \int_0^\delta (1 - u/U_s)\ \mathrm{d}y \quad \text{and} \quad \theta \equiv \int_0^\delta (u/U_s)\,(1 - u/U_s)\ \mathrm{d}y$$

Immediately apparent from Fig. 1 is the response of the boundary layer to the pressure gradient and the strong correlation between the changes in the various parameters and a value of $K = 3 \times 10^{-6}$ (the shaded vertical band indicates the region where $K > 3 \times 10^{-6}$). The shape factor H increases abruptly when K first exceeds 3×10^{-6} and peaks at a value of 2.4 as K falls back to near zero. The maximum value of the intermittency factor γ_{max} (Fig. 2) falls from 100% to near zero in the region where K exceeds 3×10^{-6}. As K falls back below 3×10^{-6}, γ_{max} recovers to 100%.

Values for $c_f/2$ determined from the wall slope of the mean velocity profile were found to be some 20% lower than the hot-film/Clauser plot values in the approach flow, and up to 70% lower than the hot-film values in the region of rapid acceleration. Based upon the consistency between the hot-film and Clauser-plot values, and other indications of the boundary-layer state, it was concluded that for the experiment reported here the wall slope does not provide an accurate estimate of wall shear stress. The friction factor peaks at essentially the same location as K and then falls to a minimum at the location where H is a maximum, at which point K has fallen almost to zero. The shape factor then drops whilst $c_f/2$ rises to a second peak practically coincident with the location where γ_{max} returns to the value 100%.

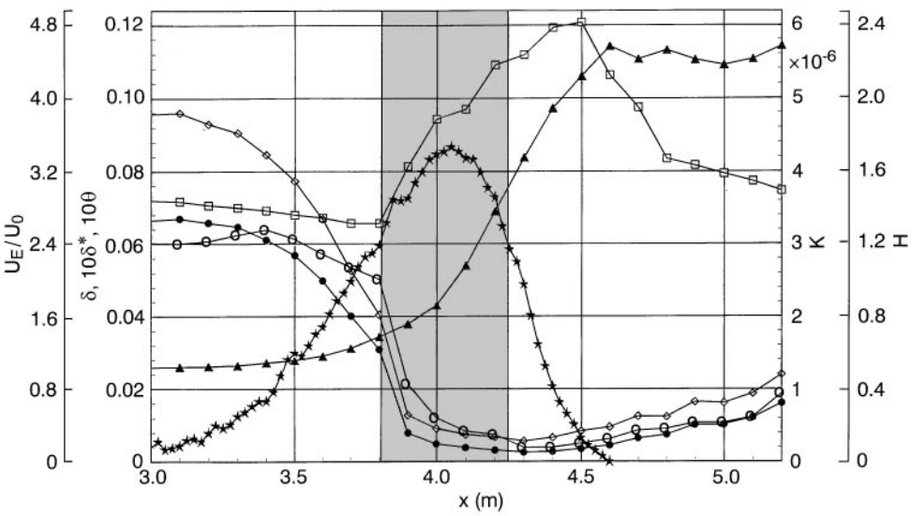

Fig. 1. Streamwise variation of K (★), U_E/U_0 (▲), δ(○), δ^* (◇), θ (●), H (□)

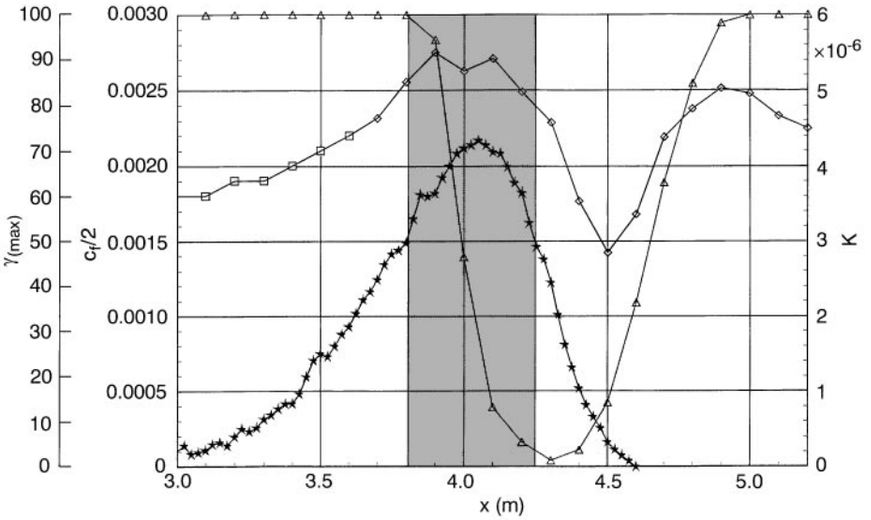

Fig. 2. Streamwise variation of K (★), $c_f/2$ (Clauser □), $c_f/2$ (hot film ◇), γ_{max} (△)

The behaviour of γ_{max} is the strongest evidence of dramatic changes in the turbulence structure of the boundary layer as a consequence of strong acceleration. Since the intermittency factor is always at its maximum either at or in the immediate vicinity of the surface, it is evident that if $K > 3 \times 10^{-6}$ the boundary layer is intermittent all the way to the surface, a feature also observed by Fiedler and Head (1966) in their laminarisation experiment. These investigators also suggested that laminarisation is indicated by a minimum in the value of the shape factor, equal to 1.28, which is very close to the value 1.31 found here at the location where γ_{max} first drops below 100%. Blackwelder and Kovasznay (1972) observed similar behaviour, with a minimum shape factor of 1.24 and intermittency levels down to 10% in the near-wall region.

The boundary layer thickness δ as well as the two integral thicknesses δ^* and θ reach minimum values at the point where K has decreased from its peak value to 3×10^{-6}. Since the momentum thickness passes through a minimum near $x = 4.3$ m, the integral momentum equation for a two-dimensional boundary layer at this location reduces to

$$c_f/2 = (2 + H)\, Re_\theta\, K$$

The measured values for H, Re_θ and K at $x = 4.3$ m are 2.23, 221, and 2.44×10^{-6}, respectively, which leads to $(2+H)Re_\theta K = 2.28 \times 10^{-3}$ in excellent agreement with the measured value (hot film) of $c_f/2 = 2.29 \times 10^{-3}$. A more general check on two-dimensionality, in which the measured values of c_f, H and K are used in the integration of the integral momentum equation, is less satisfactory. The reason for the discrepancy between the hot-film measurements and the calculated c_f values is unclear. It is possible that the c_f values in the recovery region ($x > 4.3$ m) are increasingly in error or the flow is increasingly non two-dimensional, but there seems to be no reason for the c_f values to be more inaccurate in the recovery region than was the case upstream and there is also no obvious reason why the flow should depart from two dimensionality in this region. Although, as will be seen, the turbulence intensity increases rapidly once the pressure gradient is relaxed, and it might be thought that this could explain the discrepancy, the normal-stress term $1/U_E^2\ (\mathrm{d}/\mathrm{d}x) \int_0^\infty u'^2\, \mathrm{d}y$ turns out to be an order of magnitude smaller than $c_f/2$. Another possible explanation involves the pressure variations across the boundary layer associated with streamline curvature. Even though streamline curvature is considerably larger than is usually the case for a flat-plate boundary layer, the ratio of boundary-layer thickness to streamline radius of curvature is still much less than 10^{-2} and so cannot explain the discrepancy. Whilst the uncertainty over the two-dimensionality of the flow is unsatisfactory, this does not invalidate the general conclusions of this investigation.

3.2 Mean velocity profiles

Mean velocity profiles in the form u/U_E versus the non-dimensional stream function ψ/υ are shown in Fig. 3, separated for clarity into two sets: (a) 3.1 m $< x <$ 4.3 m (increasing K), and (b) 4.3 m $< x <$ 5.2 m (decreasing K). The symbols used to denote the x location of each velocity profile are listed in Table 1, and correspond to the profiles of quantities plotted in Figs. 3–8. The stream function has two key advantages over the distance y as the ordinate choice. First, it facilitates following the development of the flow structure along streamlines. Secondly, ψ/υ is in effect a wall variable since

$$\psi/\upsilon \equiv \int_0^y u\, \mathrm{d}y/\upsilon \equiv \int_0^{y^+} u^+\, \mathrm{d}y^+$$

so that in the sublayer

$$\psi/\upsilon = y^{+2}/2.$$

The boundary layer shows the usual progressive development with increasing thickness and hence ψ_δ, the stream function at the boundary-layer edge, until the onset of the acceleration at about $x = 3$ m. The normal development is arrested at about $x = 3.1$ m and, as seen in Fig. 3a, the profile becomes progress-

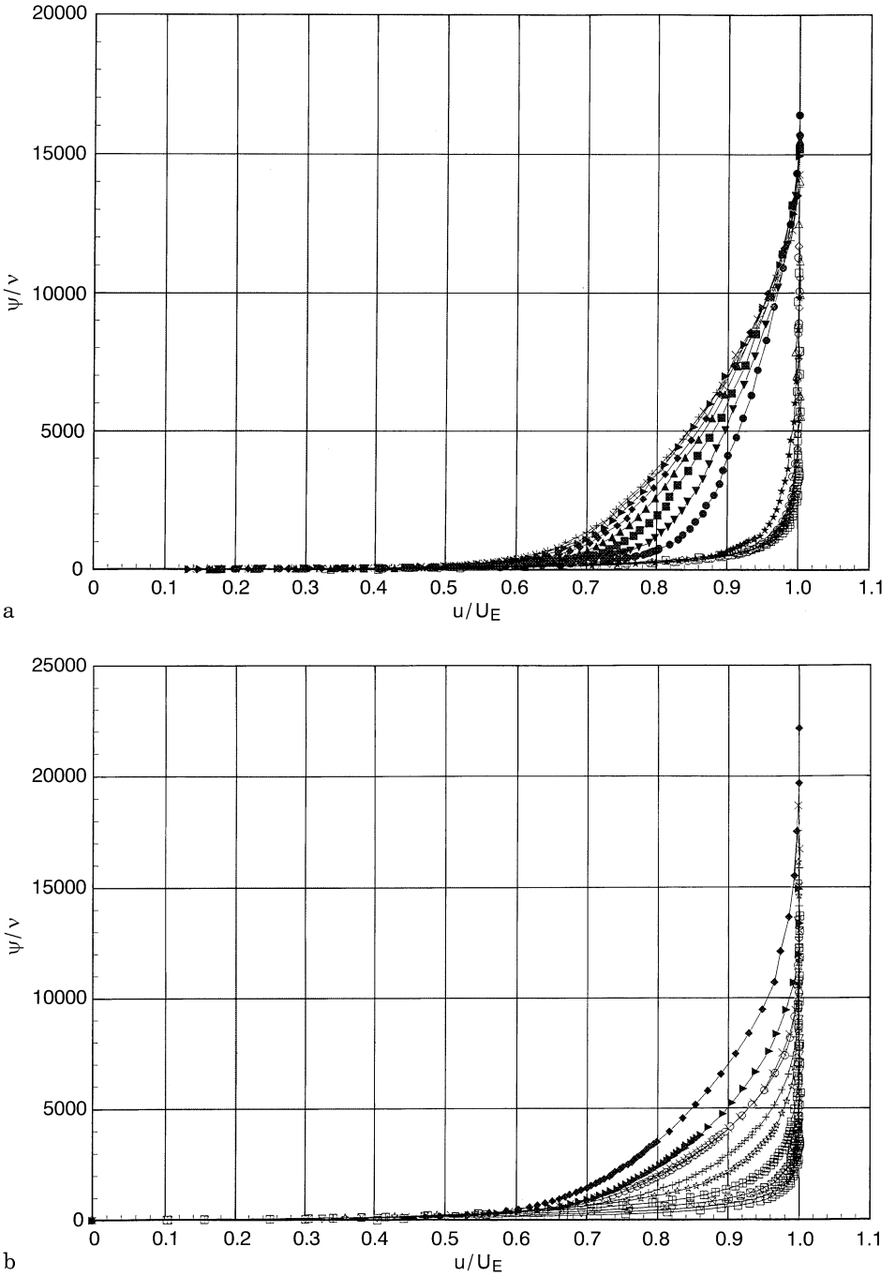

Fig. 3a,b. Mean velocity profiles u/U_E vs. ψ/υ. **a** $3.1 \leqslant x \leqslant 4.3$ m, **b** $4.3 \leqslant x \leqslant 5.2$ m

Table 1. Symbols used in Figs. 3—8

Symbol	x (m)	Symbol	x (m)
+	3.1	◇	4.2
×	3.2	□	4.3
▶	3.3	▽	4.4
◆	3.4	■	4.5
▲	3.5	■	4.6
■	3.6	☆	4.7
▼	3.7	+	4.8
●	3.8	×	4.9
★	3.9	O	5.0
O	4.0	▶	5.1
△	4.1	◆	5.2

ively fuller up to $x = 3.8$ m (the first location of $K = 3 \times 10^{-6}$) at which point there is an abrupt change in the profile consistent with the shape-factor increase observed in Fig. 1. Beyond $x = 4.3$ m (Fig. 3b), at which point K has fallen to about 2×10^{-6}, the profile progressively recovers as the boundary layer again thickens. In the region of high acceleration a number of factors conspire to make it even more difficult than usual to specify a thickness δ for the boundary layer. In part, as already noted, this is because the outer flow itself is not consistent with a uniform velocity but exhibits a near linear variation with distance from the surface. A less obvious factor is associated with the acceleration of fluid initially in the outer region of the boundary layer. To illustrate the point, consider

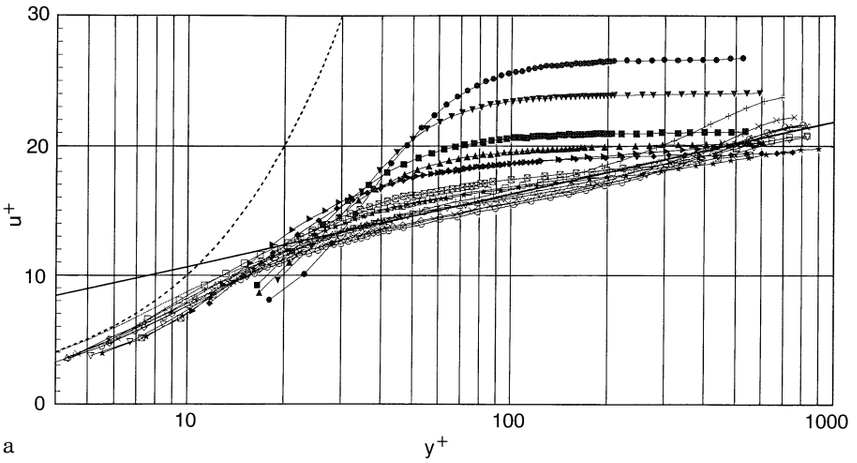

a

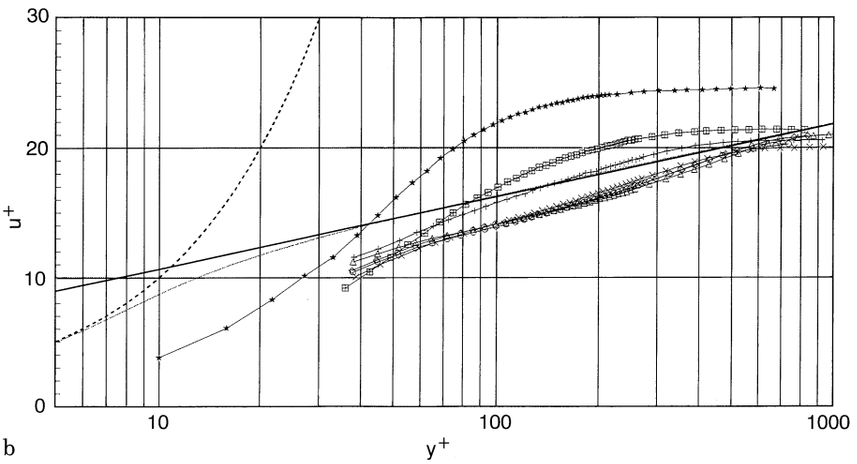

b

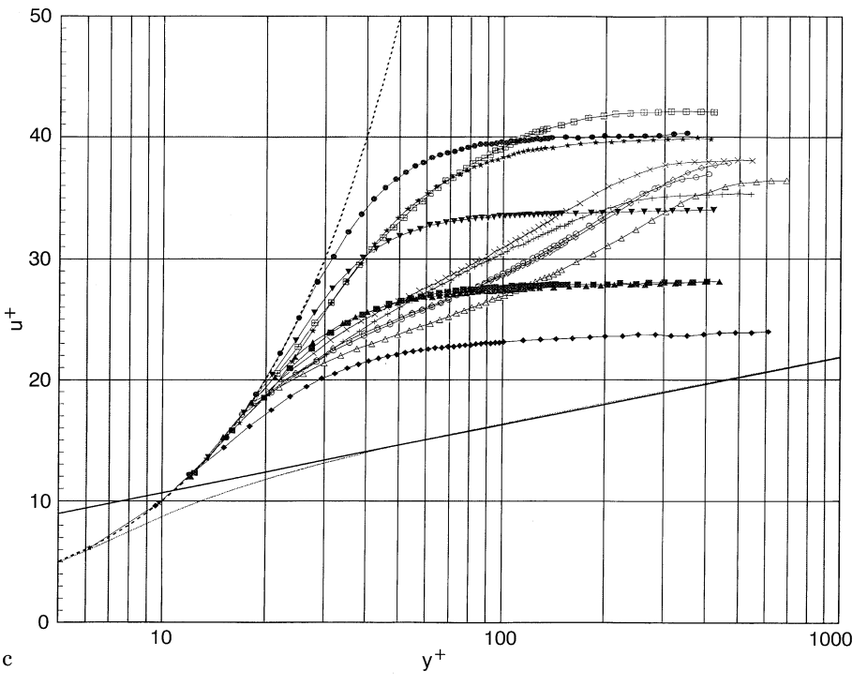

c

Fig. 4a–c. Mean velocity profiles u^+ vs. y^+ (including $u^+ = y^+$, $u^+ = (1/\kappa) \ln y^+ + B$ and Spalding's (1964) formula). **a** $3.1 \leqslant x \leqslant 4.5$ m, **b** $4.6 \leqslant x \leqslant 5.2$ m, **c** $4.1 \leqslant x \leqslant 5.2$ m using the near-wall gradient for τ_s

a location near the edge of the boundary layer upstream of the acceleration where $u/U_E = 0.99$. Since U_E increases by a factor of 4.4 between $x = 3.0$ and 4.5 m (see Fig. 1), a simple inviscid estimate reveals that u must increase such that u/U_E reaches the value 0.9994, which would place it well outside a boundary layer specified by $u/U_E = 0.99$. The same estimate shows that the latter value downstream corresponds to an upstream value of $u/U_E = 0.826$, further illustrating the point. What this argument reveals is that whatever the influence on the turbulence structure of a boundary layer, it is inevitable that a strong favourable pressure gradient will cause the velocity profile to fill out and assume a more laminar appearance. Fortunately, this second difficulty in specifying a boundary-layer thickness does not affect the evaluation of the integral thicknesses.

The mean velocity-profile data in wall coordinates (u^+ versus ln y^+, Fig. 4) have been separated for clarity into two slightly different sets to those of Fig. 3. In the zero pressure gradient region the profiles for the turbulent core show excellent agreement with the universal profile represented $u^+ = \ln y^+/\kappa + B$, with $\kappa = 0.41$ and $B = 5.0$. Also shown in Fig. 4 is $u^+ = y^+$ to represent the viscous sublayer and Spalding's (1964) formula for the entire near-wall region

$$y^+ = u^+ + e^{-\kappa B}\,[e^{\kappa u^+} - 1 - \kappa u^+ - (\kappa u^+)^2/2 - (\kappa u^+)^3/6]$$

One key reason why the wall slope failed to produce acceptable values for $c_f/2$ is evident from Fig. 4: the data extend only to $y^+ \approx 4$, which is not sufficiently small.

The progressive departures from the universal near-wall $u^+(y^+)$ form evident in Figs. 4a and b are consistent with previous studies of accelerating turbulent flows. Three particular points are noteworthy. First, the greatest deviation from the universal form occurs at $x = 4.5$ m where $K = 3.2 \times 10^{-7}$ well after the location of the peak value of K at $x = 4.1$ m. Secondly, the flow overshoots the log law in the return to zero pressure gradient conditions, although the appearance of the profiles for $x = 4.9$–5.2 m indicates that the data could be forced to conform to the logarithmic law with a reduced value for $c_f/2$. In fact, this suggestion is partially supported by the Clauser plots for these profiles shown in Fig. 5: for $x = 5.2$ m, a logarithmic law of limited extent can be identified corresponding with $c_f/2 = 0.00176$, 21% lower than the hot-film value of 0.00225. However, for the other three profiles (at $x = 4.9$, 5.0 and 5.1 m) it is quite clear that the return to a normal turbulent boundary layer is far from complete. As will be seen shortly, the turbulence data also lead to this conclusion. Thirdly, as seen in Fig. 4(c), the use of the wall slope to determine $c_f/2$ inevitably leads to a much better collapse of the data on $u^+ = y^+$ in the very near wall region, as was observed by Blackwelder and Kovasznay (1972). As noted earlier, however, the values of $c_f/2$ so determined are up to 70% lower than the hot film values and less consistent with other indicators, including the two-dimensional momentum equation.

3.3 Intermittency

As already noted, the near-wall intermittency falls below 100% for $x > 3.8$ m, the location at which K first exceeds 3×10^{-6}, and then falls rapidly to near zero at $x = 4.3$ m, well beyond the location where the pressure gradient parameter peaks. As can be seen in Fig. 6a, the intermittency at any x-location decreases monotonically with ψ/υ (except for the very near wall behaviour at $x = 3.9$ and 4.0 m), and is practically equal to zero across the entire boundary layer at $x = 4.3$ m: the boundary layer at this location can be regarded as completely laminarised. The streamwise increase in intermittency following relaxation of the pressure gradient (Fig. 6b) is slightly less rapid in the near wall region than the decrease produced by the acceleration, but more rapid in the boundary layer core. Careful scrutiny of the intermittency curves reveals a significant difference between the final distribution at $x = 5.2$ m and the distribution at $x = 3.1$ m for which the value of ψ_δ/υ is roughly comparable: over the outer part of the boundary layer ($\psi_\delta/\upsilon > 6000$), with approach to the free stream, the intermittency values are progressively greater for the recovered flow than for the approach flow. This difference is a further indicator that the flow has not fully recovered even at $x = 5.2$ m.

3.4 Turbulence intensity

The turbulence intensity profiles are presented in Figs. 7 and 8 in two different forms: u'/U_E versus ψ/υ and u'/U_0 versus ψ/υ.

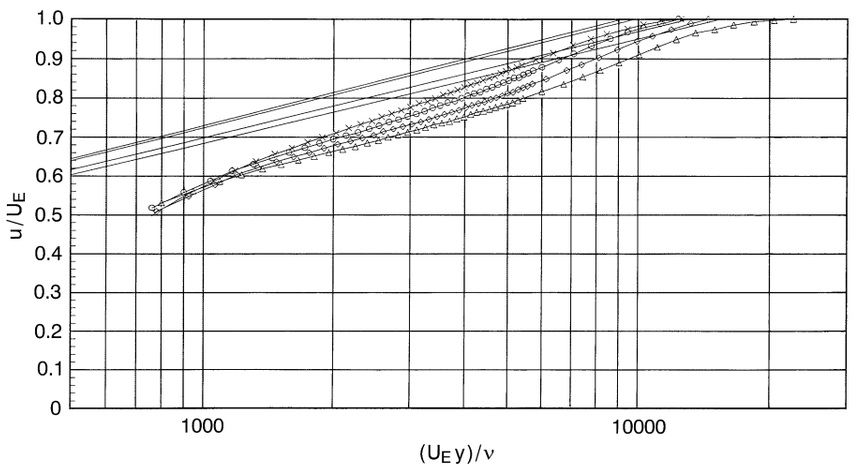

Fig. 5. Mean velocity profiles in Clauser plot form u/U_E vs. $U_E y/\upsilon$ $4.1 \leqslant x \leqslant 5.2$ m

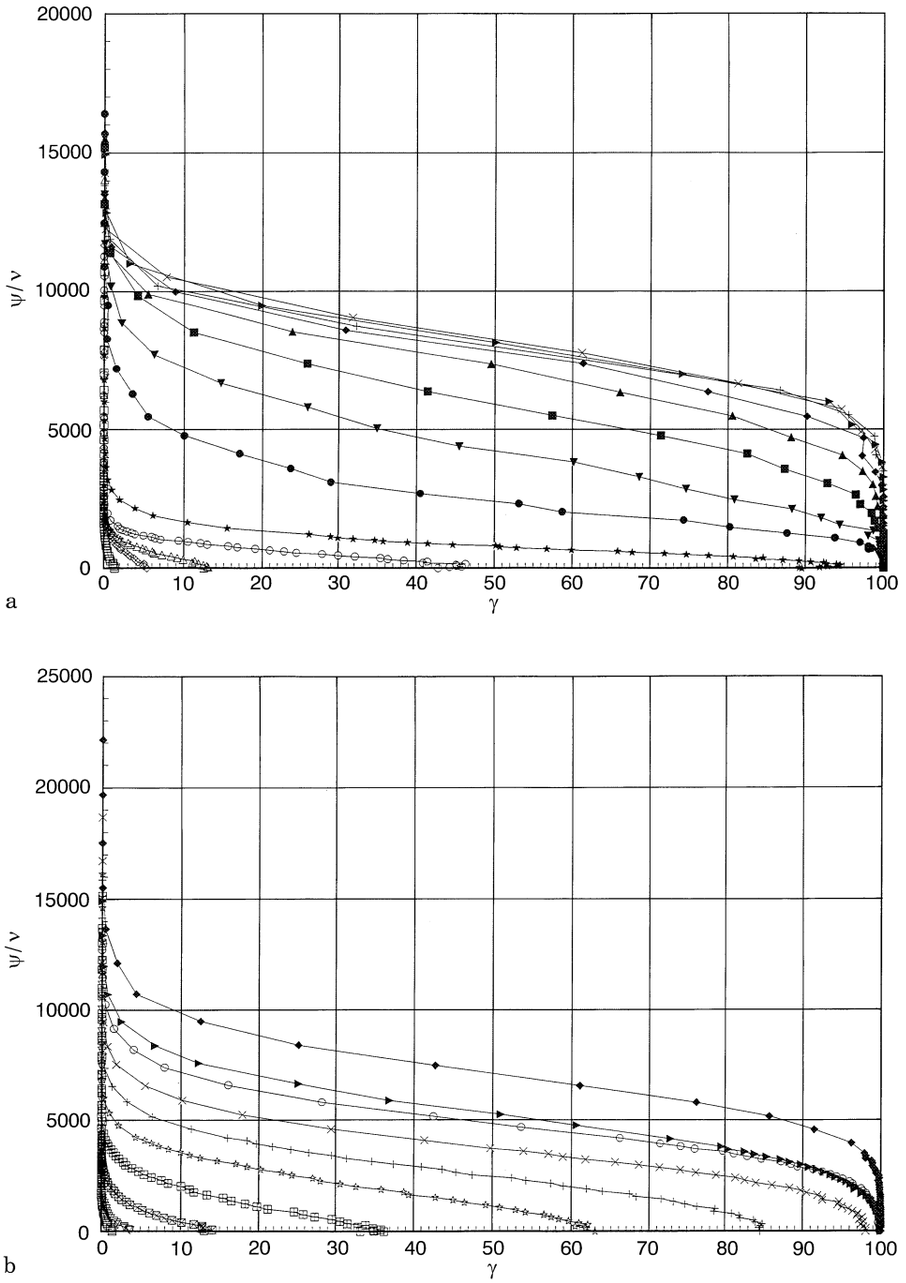

Fig. 6a–c. Intermittency γ vs. ψ/υ. **a** $3.1 \leqslant x \leqslant 4.3$ m, **b** $4.3 \leqslant x \leqslant 5.2$ m

In addition, Figs. 7b and d show expanded views of the near-wall behaviour ($\psi/\upsilon \leqslant 5000$). In the inner region of the boundary layer ($\psi/\upsilon < 400$), the turbulence intensity increases along the streamlines essentially in proportion to the free stream velocity U_E (Fig. 7b) until K reaches about 3.6×10^{-6} at $x = 3.9$ m, somewhat beyond the location at which departures of the mean velocity from the logarithmic law were evident (Fig. 4a). Since U_E has increased from 4 to about 6 m/s in this region, the turbulence intensity has increased in absolute terms along each streamline by about 50%. This increase is more evident in Fig. 8a in which u' has been normalised with the approach-flow free-stream velocity U_0 (i.e. 4 m/s). In the outer region the relative turbulence intensity u'/U_E falls monotonically throughout the acceleration region (Fig. 7a) but, as Fig. 8a shows, u' is in fact effectively frozen near the edge of the boundary layer and falls slightly in mid boundary layer. These results are similar to those reported by Blackwelder and Kovasnay (1972) although the decay of u' in mid boundary layer is less clear in their investigation.

Figs. 7c, d and 8b reveal the near-wall recovery of u' for $x > 4.3$ m, $K < 3 \times 10^{-6}$ to be far more complex than the straightforward transition of a laminar boundary layer. This observation is hardly surprising in the light of the turbulence levels remaining in the laminarised boundary layer (i.e. at $x = 4.3$ m where the intermittency was found to be practically zero throughout the boundary layer). The first indication of

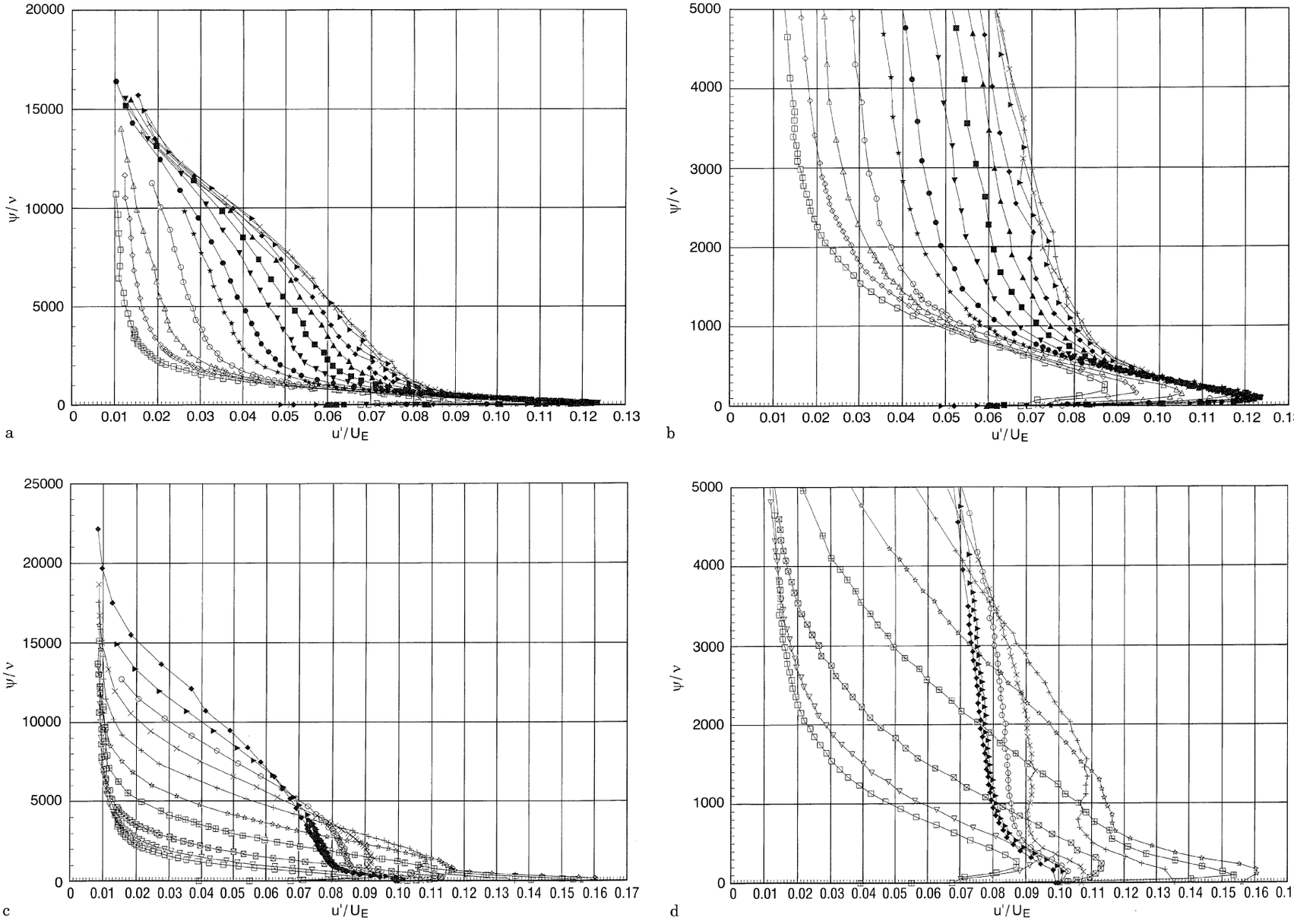

Fig. 7a–d. Turbulence intensity u'/U_E vs. ψ/υ. **a** $3.1 \leqslant x \leqslant 4.3$ m, **b** near-wall detail $3.1 \leqslant x \leqslant 4.3$ m, **c** $4.3 \leqslant x \leqslant 5.2$ m, **d** near-wall detail $4.3 \leqslant x \leqslant 5.2$ m

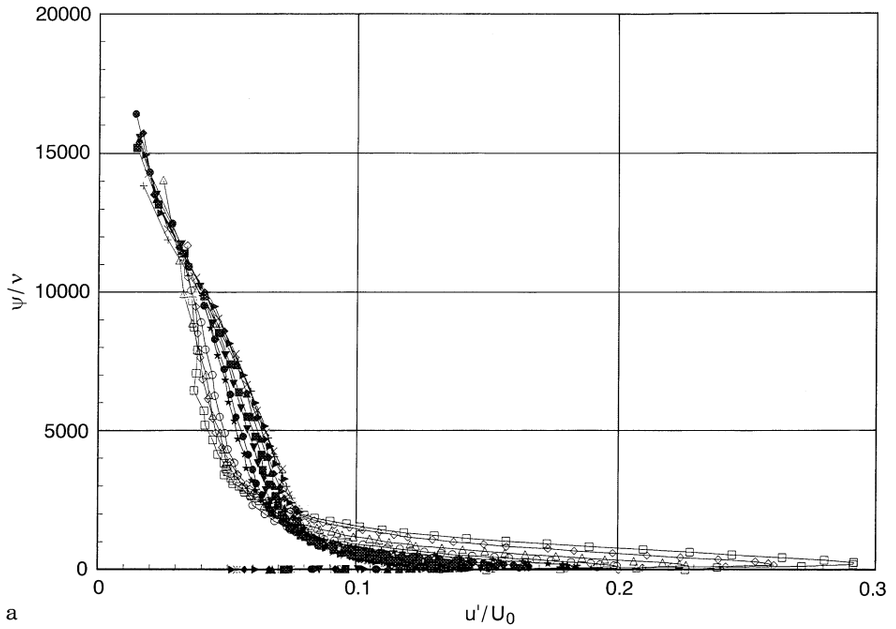

a

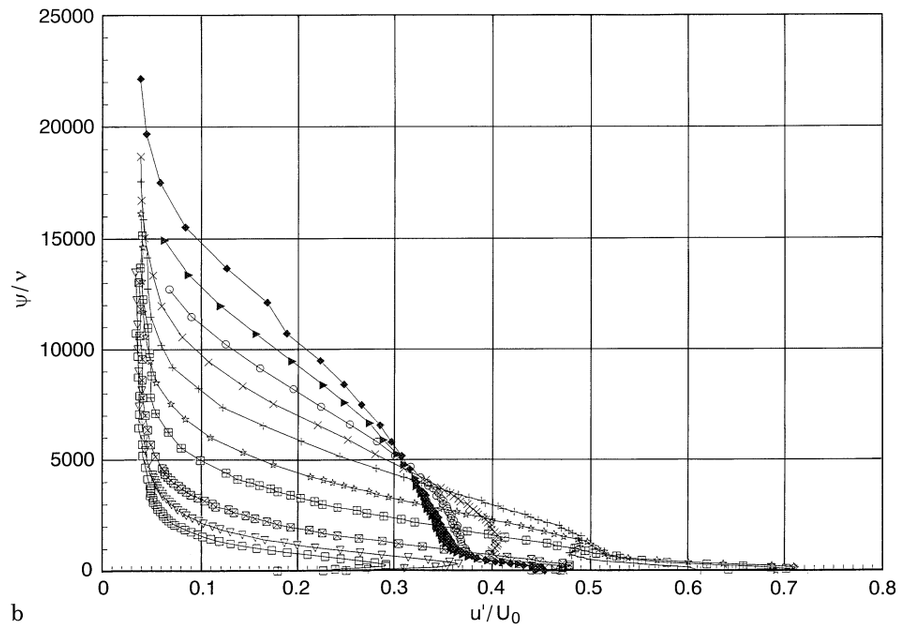

b

Fig. 8a,b. Turbulence intensity u'/U_0 vs. ψ/υ. **a** $3.1 \leqslant x \leqslant 4.3$ m, **b** $4.3 \leqslant x \leqslant 5.2$ m

this complexity is at $x = 4.5$ m where a slight inflexion appears in the u' distribution at about $\psi/\upsilon = 400$. This inflexion continues to develop and move away from the surface until it disappears at $x = 4.9$ m. What is also unusual is that beyond $x = 4.7$ m the near-wall turbulence intensity shows a rapid decrease in level, initially in relative terms (i.e. u'/E_E) and then in absolute terms (u'/U_0). This process comes to an end at $x = 5.1$ m, suggesting that a "normal" zero pressure gradient state has been reached. In fact, the final distribution at $x = 5.2$ m is considerably different from what would be expected of a normal turbulent boundary layer with a peak value of u'/U_E about 30% too low. The outer region beyond $x = 4.5$ m reveals significant increases in u' (see Fig. 8b) along streamlines indicating that once K has fallen to a negligible level, turbulence production resumes throughout the boundary layer.

4 Discussion

The experimental mean velocity and intermittency values, presented in the previous section, clearly describe a re-laminarising flow between $x = 3.8$ and 4.3 m, which suggests that the $u'v'$ Reynolds stress within the boundary layer decreases rapidly within this region. However, in contrast, the

measured turbulence intensity u' shows no significant decrease. To understand this result it is necessary to consider turbulence within the relaminarising boundary layer in greater detail.

There would appear to be two requirements for a turbulent boundary layer to relaminarise: firstly, the generation of turbulence must be suppressed and, secondly, the Reynolds stresses due to existing turbulence must decay to negligible levels.

Figure 8a shows that the absolute values of fluctuation level do not decay by more than about 30% for the outer streamlines ($\psi/\upsilon > 2000$) whilst closer to the wall fluctuation levels increase by up to 100%. It is therefore the 4.4 fold increase in mean velocity that leads to the observed decrease in turbulence level in Fig. 7a. The decrease closer to the wall ($\psi/\upsilon < 500$) is modest and only commences following the start of relaminarisation at $x = 3.9$ m and is regarded as a consequence of relaminarisation rather than the cause of it. It would appear that the nature of the turbulence is altered in the acceleration region up to $x = 3.9$ m in such a way that the Reynolds stresses associated with it are reduced to negligible levels.

It is reasonable to assume that if the amplitude of the turbulence has not altered significantly along a streamline then neither has its frequency content and any decay will be greatest at the highest frequencies. The fluctuations associated with momentum transport (i.e. significant Reynolds stresses) within the boundary layer will have frequencies greater than $U_E/2\pi\delta$. The value of $U_E/2\pi\delta$ increases from 11 Hz at $x = 3.1$ m to 45 Hz at $x = 3.9$ m and 533 Hz at $x = 4.3$ m. Therefore the bulk of the turbulence generated in the boundary layer prior to acceleration will be at frequencies which are too low to cause significant Reynolds stresses within the laminarising boundary layer.

An interesting region of the boundary layer in relaminarisation is that which exists, in the present study, between $\psi/\upsilon = 3000$ and 14 000. As mentioned previously although this fluid may have a value of u'/U_E as low as 0.826 (for $\psi/\upsilon = 3000$, $x = 3.1$ m) in the boundary layer prior to acceleration, it will achieve $u/U_E > 0.99$ after acceleration and from an experimental point of view is practically indistinguishable from the freestream. Narasimha and Sreenivasan (1973) referred to this region as the outer layer and demonstrated that although the flow is essentially inviscid, it is rotational. More importantly the turbulence level will have been enhanced whilst the fluid was in the turbulent boundary layer prior to acceleration and will only decay slowly within the outer layer. This is therefore the most likely reason for the higher intermittency values observed for $\psi/\upsilon > 6000$ in the recovered flow $x = 5.2$ m compared with the approach flow $x = 2.2$ m. The enhanced turbulence level in the freestream above the laminarised layer may also promote earlier retransition.

5 Conclusions

The results of the laminarisation experiment reported here are consistent with previous work, particularly that of Blackwelder and Kovasznay (1972). A clearer picture than existed hitherto has emerged of a number of aspects of the fundamental characteristics of the boundary layer. The response of both the mean velocity profile and the turbulence structure to the pressure gradient is found to be initially progressive but to show an abrupt change when K exceeds a critical value. The precise magnitude of this critical value is likely to depend upon the initial value of Re_θ, but not the qualitative behaviour of such parameters as H, $c_f/2$ and the near-wall value of γ. The differing responses of the near-wall and outer regions of the boundary layer are also clearly confirmed.

Although it seems reasonable to refer as laminar to a boundary layer with near-zero values of intermittency, in fact the levels of turbulence intensity within the boundary layer remain high. The explanation for what appears to be a contradiction is that the turbulence which originated in the relatively thick boundary layer upstream is dominated by frequencies much lower than would be produced in the thin boundary layer which results from the pressure gradient. The intermittency algorithm acts effectively as a high pass filter and thus the low levels of γ indicate that little such high-frequency turbulence is produced and it is in this sense that the boundary layer is laminar.

The subsequent development of the boundary layer once the pressure gradient is relaxed reveals a minimum in $c_f/2$ just upstream of the location of $K = 0$, with very steep gradients around the minimum. Even though the near-surface value of γ returns to unity following relaxation of the pressure gradient, other indicators suggest that the boundary layer as a whole is still far from the fully developed state.

In the region downstream of the severe pressure gradient, the near-wall gradient of the mean velocity to estimate the wall shear stress τ_s leads to values considerably lower than those obtained from surface hot-film measurements. This difference in the τ_s values leads to a very different impression of the state of the boundary layer based upon the mean velocity profiles in wall-coordinate form. The hot-film results are seen as the more reliable.

References

Ashill PR; Betts CJ (1993) A study of the flow around the leading edge of a highly-swept wing in a low-speed wind tunnel. ASME FED 151: 221–227

Blackwelder RF (1995) Private communication

Blackwelder RF; Kovasznay L (1972) Large-scale motion of a turbulent boundary layer during relaminarization. J Fluid Mech 53: 61–83

Bradshaw P; Pankhurst R (1964) The design of low-speed wind tunnels. Prog Aero Sci 5: 1–69

Cimbala JM; Park WJ (1990) A direct hot-wire calibration to account for ambient temperature drift in incompressible flow. Exp. Fluids 8: 299–300

Clauser FH (1954) Turbulent boundary layers in adverse pressure gradients. J Aero Sci. 21: 91–108

Fasihfar A (1992) Mechanisms of boundary layer transition. PhD thesis, University of Liverpool

Fiedler H; Head MR (1966) Intermittency measurements in the turbulent boundary layer. J Fluid Mech 25(4): 719–735

Gibson MM (1960) The design of a wind tunnel for boundary layer research. PhD thesis, University of Liverpool

Johnson MW (1988) Boundary layer transition measurements using a hot wire anemometer and digital signal processing. Internal Report FM/122/88, Dept of Mech Eng, Univ of Liverpool

Jones W; Launder BE (1972) The prediction of laminarization with a two-equation model of turbulence. Int J Ht Mass Trans 15: 301–314

Lee T; Budwig R (1991) Two improved methods for low-speed hot-wire calibration. Meas Sci Technol 1: 643–646

Narasimha R; Sreenivasan KR (1973) Relaminarisation in highly accelerated turbulent boundary layers. J Fluid Mech 61: 417–447
Patel VC (1965) Calibration of the Preston tube and limitations on its use in pressure gradients, J Fluid Mech 23: 185–208
Shaw R; Hardcastle JA; Riley S; Roberts CC (1985) Recording and analysis of fluctuating signals using a microcomputer. Measurement 3: 33–39
Spalding DB (1961) A single formula for the law of the wall. J Appl Mech 28: 455–457
Sreenivasan KR (1982) Laminariscent, relaminarizing and retransitional flows. Acta Mech 44: 1–48